The Effects of Clay Dispersion on the Mechanical, Physical, and Flame-Retarding Properties of Wood Fiber/Polyethylene/Clay Nanocomposites

Yoon H. Lee,[1] Takashi Kuboki,[2] Chul B. Park,[2] Mohini Sain,[1] Marianna Kontopoulou[3]

[1]*Centre for Biocomposites and Biomaterials Processing Faculty of Forestry, University of Toronto, Ontario, Canada M5S 3B3*
[2]*Microcellular Plastics Manufacturing Laboratory, Department of Mechanical and Industrial Engineering, University of Toronto, Toronto, Ontario, Canada M5S 3G8*
[3]*Department of Chemical Engineering, Queen's University, Kingston, Ontario, Canada K7L 3N6*

Received 12 April 2009; accepted 31 December 2009
DOI 10.1002/app.32045
Published online 21 May 2010 in Wiley InterScience (www.interscience.wiley.com).

ABSTRACT: In this study, nanosized clay particles were introduced into wood fiber/plastic composites (WPCs) to improve their mechanical properties and flame retardancy, which are especially important in various automotive and construction applications. A high degree of exfoliation for nanoclay in the wood fiber/high density polyethylene (HDPE) composites was successfully achieved with the aid of maleated HDPE (PE-g-MAn), through a melt blending masterbatch process. The structures and morphologies of the composites were determined using X-ray diffraction (XRD) and transmission electron microscopy (TEM), respectively. This article presents the effects of clay content and degree of clay dispersion on the mechanical and physical properties and flame retardancy of wood fiber/HDPE composites that contained a small amount of clay, in the range of 3–5 wt %. We concluded that achieving a higher degree of dispersion for the nanosized clay particles is critical to enhance the mechanical properties and the flame retardancy of WPCs when small amounts of clay are used. © 2010 Wiley Periodicals, Inc. J Appl Polym Sci 118: 452–461, 2010

Key words: clay; biofibers; polyethylene (PE); mechanical properties; flame retardance

INTRODUCTION

Because of their high specific stiffness and strength, wood fiber/plastic composites (WPCs) are a cost-effective alternative to wood and other plastic composites.[1] Wood fiber is a non-abrasive substance, which means that relatively large concentrations of this material can be incorporated into plastics without causing serious machine wear during blending and processing. In spite of their higher price, WPCs are becoming increasingly acceptable to consumers as a replacement for natural wood due to such advantages as durability, color permanence, resistance to degradation and fungal attacks, and reduced maintenance. Furthermore, adding wood fibers to plastic products makes use of waste wood. WPCs are mainly employed in building products, such as decking, fencing, rails, door and window profiles, and decorative trims. Moreover, these composites are also gaining acceptance in automotive and other industrial applications.

High density polyethylene (HDPE) is the most commonly used polymer matrix for WPCs because of its relatively low processing temperature and good processability.[2] However, hydrophobic polyethylene and hydrophilic wood fibers are naturally incompatible. The strength and impact properties of WPCs are commonly even lower than those of pure polyethylene as a result of the poor dispersion of fibers and weak interfacial interaction between the fibers and the matrix material.[3] The surface modification of fibers or use of external processing aids can facilitate the dispersion and adhesion of these fibers in the polymer matrix.[4] The most widely used coupling agents (based on reactive groups) are derivatives of either maleic anhydride or siloxanes. It has been shown that the mechanical properties of WPCs are improved when coupling agents are used in the composites.[5] However, due to the low stiffness of HDPE, the flexural and tensile moduli of the WPCs are substantially lower than those of natural wood.

Another critical drawback of WPCs is their high flammability. Improving their flame retardancy will

Correspondence to: C. B. Park (park@mie.utoronto.ca).
Contract grant sponsors: AUTO21, Consortium for Cellular and Microcellular Plastics (CCMCP), Natural Sciences and Engineering Research Council of Canada (NSERC).

thus expand the range of their applications. Halogenated flame-retardants, such as organic brominated compounds, are often used to improve the flame-retarding properties of polymers; unfortunately, these also increase both the smoke and carbon monoxide yield rates due to their inefficient combustion.[6] The other commonly used flame retardants are aluminum trihydrate (ATH), magnesium hydroxide [$Mg(OH)_2$], or intumescent systems; however, they all exhibit some significant disadvantages. For example, the application of ATH and $Mg(OH)_2$ requires a very high loading of the filler (40–60 wt %) within the polymer matrix to obtain acceptable performance levels, which yields high-density products and also adversely influences mechanical properties and processability.[7]

In this regard, nanosized clay particles, which have a much larger surface area ($\sim$ 750 m^2/g) and a much higher aspect ratio (100–1000) than conventional, macrosized fillers, are good candidates for overcoming the aforementioned drawbacks of WPCs. Adding a small amount of nanoclay (usually $\leq$5 wt %) can dramatically improve mechanical properties, thermal and dimensional stability, flame retardance, barrier properties, and many other such properties.[8–11] The key to yield these improved properties is exfoliating and completely dispersing individual platelets with high aspect ratios throughout the polymer matrix. Exfoliated nanocomposite preparation by conventional polymer processing therefore requires the occurrence of strong interfacial interactions between the polymer matrix and the clay, as well as the generation of sufficient shear forces to make the entire surface of the clay layers available for the polymer. This is readily achieved with highly polar polymers like polyamides. However, for many commercially important, nonpolar or weakly polar polymers such as polyethylene (PE), polypropylene (PP), and polystyrene (PS), natural incompatibility with the polar clay surface poses a significant challenge to achieve complete exfoliation of nanoclays.

The most common approaches to produce polyolefin nanocomposites involve in-situ polymerization and melt blending.[12] The latter is more convenient from an industrial standpoint because it does not employ organic solvents and can be easily combined with conventional polymer processes like extrusion and injection molding. For melt blending in PE/clay systems, PE functionalized via the grafting of maleic anhydride (PE-g-MAn) or acrylic acid, as well as block-copolymers of ethylene with monomers containing acid groups, has been used to overcome problems associated with poor interfacial interactions between polymers and nanoclays.[13–26] Functional groups such as succinic anhydride and acids increase the interactions between the clay surface and the polymer chain, and create a favorable enthalpy for the compound to mix with the polymer matrix. Therefore, it may be possible to use PE-g-MAn as a coupling agent for wood fiber/PE composites as well as for PE/clay nanocomposite systems, simplifying fabrication of the composites.

Both WPCs and polymer/clay nanocomposites have been explored extensively, but always separately.[27,28] Very few researchers have tried to combine wood fiber, nanoclay, and PE to produce WPCs with improved performance capacities. Guo et al.[27] showed that the addition of intercalated clay particles affects favorably the cell morphology of metallocene PE/wood fiber composites in the extrusion foaming using a CBA. They also demonstrated that using a small amount of well-dispersed nanoclay (i.e., 0.1–0.5 wt %) can improve the flame retarding properties of wood fiber/HDPE composites.[28] On the other hand, the adhesion between wood fiber and clay particles, which are hydrophilic in nature, is at least as strong as the adhesion between fibers; hence, the clay exfoliation in WPCs necessary to improve properties may be difficult to achieve.

The objective of this study is first to achieve good exfoliation of nanoclay in WPCs. This exfoliation is performed in a two-step process: creation of a PE-g-MAn–based nanoclay masterbatch and then dilution of this masterbatch with pure HDPE for a fixed amount of wood fiber. The purpose of this process is to obtain clay exfoliation in PE-g-MAn with high molecular weight and to dilute with low molecular HDPE at fixed amount of wood fiber while preserving the exfoliation obtained in the nanoclay masterbatch. From an economic point of view, it is desirable to make the masterbatch as concentrated in nanoclay as possible. The resulting products are then compared to equivalent nanocomposites prepared, with no masterbatch, by direct melt processing from pure HDPE, PE-g-MAn, wood fiber, and clay. The second objective of this study is to investigate the effects of clay dispersion (i.e., intercalated versus exfoliated) on the mechanical, thermal, rheological, and flame retarding properties of wood fiber/HDPE/clay (1–5 wt %) nanocomposites prepared by two different melt blending processes.

EXPERIMENTAL

Materials

HDPE (SCLAIR 2710, Nova Chemicals), which has a melt flow index (MFI) of 17 g/10 min and a density of 0.95 g/cm^3, was used as a matrix in this experiment. Dupont Canada contributed HDPE grafted with maleic anhydride (PE-g-MAn, Fusabond MB100D, MFI = 2.0), which was used as an interface modifier. The wood fiber used was standard

TABLE I
Formulation of the Composites Used (wt %) in the Experiment

Sample	HDPE	Wood-fiber	PE-g-MAn	Clay
MB10			90	10
1	61	30	9	0
2	60	30	9	1
3	60	30	9	1 (10% of MB10)
4	43	30	27	0
6	40	30	27	3
7	40	30	27	3 (30% of MB10)
8	25	30	45	0
10	20	30	45	5
11	20	30	45	5 (50% of MB10)

softwood (pine) grade 12,020 (average particle size 75–125 μm), and was supplied by American Wood Fibers. Clay modified with dimethyl dehydrogenated tallow alkyl ammonium (Cloisite 20A, Southern Clay Products) was employed as a layered silicate. The organoclay used in the study has a specific gravity of 1.77 g/cm^3 and a d-spacing of about 2.6 nm. The wood fiber, the organoclay, and the PE-g-MAn were all dried at 60°C for 24 h prior to compounding.

Preparation of composites

To compare samples from the standpoint of clay dispersion, two different mixing procedures were used: masterbatch and direct melt blending. In the masterbatch mixing process, a masterbatch was first prepared by melt-blending the PE-g-MAn and the organoclay (weight ratio of 90 : 10) using a high-shear kinetic mixer (K-mixer, W&P Gelimat) at 3200 rpm. This mixing encouraged a chemical interaction between the hydroxyl groups present on the nanoclay and the maleated PE. The maleic anhydride (MA) groups in the maleated PE reacted with the hydroxyl groups (OH) on the surface of the nanoclay so that ester bonding and/or hydrogen bonding occurred between the maleated PE and the nanoclay, which dispersed the nanoclay particles uniformly throughout the wood fiber composites. The melt-blended bundles were discharged at a preset temperature of 170°C and were cut into small granules by a granulator (C. W. Brabender). The masterbatch granules were dry-blended with HDPE and wood fiber so that the final material compositions reached the values recorded in Table I. The organoclay contents were varied between 1 and 5 wt %. For all composites, the weight ratio of PE-g-MAn to organoclay was fixed at 9.0, which has been shown by our previous studies to be optimum for promoting exfoliation of organoclay in PE-g-MAn nanocomposites. The blends were compounded first in a K-mixer, then further in a counter-rotating intermeshing twin-screw extruder (C. W. Brabender: Model D6/2, 7 : 1 L/D, 42 mm screw diameter) with a barrel temperature profile ranging from 140°C to 160°C between the feed zone and the die zone, at a screw speed of 70 rpm. The mixture was plasticized and uniformly mixed by the intensive counter-rotation of the twin screws. The extrudate was cooled with blowing air and subsequently pelletized.

In the direct mixing process, wood fiber, HDPE, PE-g-MAn, and organoclay were added to the kinetic batch mixer at the same time, where they were compounded and subsequently melt-blended in a counter-rotating intermeshing twin-screw extruder. The compounded composites were dried at 90°C for 12 h. The dried pellets were then injection-molded in an ENGEL injection-molding machine to produce ASTM-standard specimens.

Characterization of the nanoclay structure

The clay dispersion in the composites was characterized by wide-angle X-ray diffraction (XRD) and transmission electron microscopy (TEM). XRD was conducted with a Siemens D5000 diffractometer that used Cu Kα radiation ($\lambda = 1.5418$ Å) with a Kevex solid-state detector. Measurements were performed at 50 kV and 35 mA. The data was recorded in the reflection mode in the range $2\theta = 1.0–10°$ using the STEP scan method; the step size was 0.02° and the counting time was 2.0 seconds per step. Materials with a periodic structure like the layered silicate clay typically show characteristic (001) diffraction peaks related to the spacing of the layers in accordance with Bragg's law, $\lambda = 2d_{001}\sin\theta$, where λ is the wavelength of the radiation, d_{001} is the interlayer spacing, and 2θ is the diffraction angle.

For the TEM analysis, the specimens were cut to produce an ultra-thin section of thickness 70 nm using a microtome with a diamond knife. The clay dispersion was observed using a Hitachi HD-2000 TEM at 200 kV.

Crystallization behavior

The crystallization and melting temperatures and crystallinity of the samples were measured using differential scanning calorimetry (DSC, model TA 2910) with a thermal analysis data station. Each sample was heated to 180°C at a rate of 10°C/min. The samples were then allowed to cool down at a rate of 10°C/min. Then, a second heating scan was carried out at a rate of 10°C/min. The sample weights were 5–7 mg. Thermal properties such as melting temperature (T_m), crystallization temperature (T_c), and heat of fusion (ΔH_{exp}), were determined from the DSC thermograms. The degree of crystallinity (χ_c) of HDPE was evaluated according to the following relationship:

$$\chi_C = \frac{\Delta H_{\text{exp}}}{\Delta H^*} \times \frac{1}{W_f} \quad (1)$$

where ΔH_{exp} is the experimental heat of fusion determined from DSC; ΔH^* is the heat of fusion of the fully crystalline HDPE (293 J/g); and W_f is the weight fraction of HDPE in the composites. Three measurements per sample were taken to confirm the repeatability of the data.

Rheological characterization

The samples were subjected to oscillatory shear in a Dynamic Stress Rheometer (Rheometric Scientific SR-200) with parallel plates (diameter 25 mm) and at a gap of 1.0 mm. In all cases, dynamic stress sweeps were performed initially to define the limits of the linear viscoelastic regime. Dynamic frequency sweep experiments were then conducted to measure the storage modulus (G'), loss modulus (G''), and complex viscosity (η^*) over the frequency range 0.1–100 rad/s at 180°C. All measurements were performed under nitrogen to prevent polymer degradation and moisture absorption.

Mechanical property testing

The tensile and flexural properties were determined using a standard computerized testing machine (Zwick Z100) with a load cell of 10 kN capacity. The tensile properties were calculated in accordance with the ASTM D638 procedure; five specimens at a cross-head speed of 10 mm/min were employed. The flexural properties were measured in accordance with ASTM D790 using five specimens in a three-point bending mode at a cross-head speed of 13.5 mm/min and a span width of 53 mm. Izod impact tests followed the ASTM D256 procedure using a pendulum-type impact machine on five notched specimens.

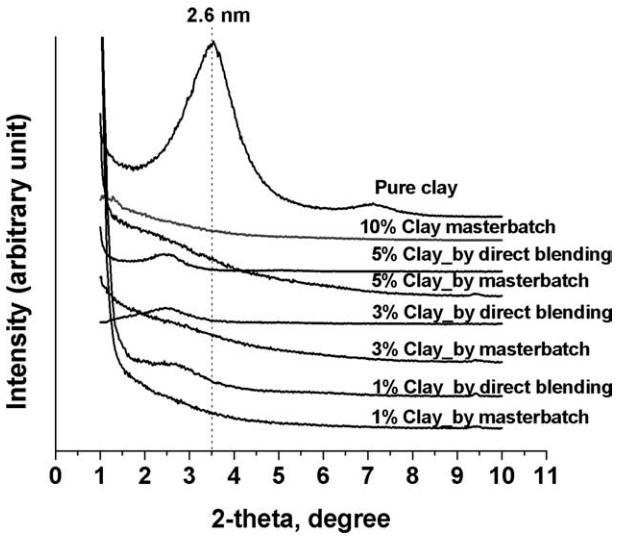

Figure 1 XRD patterns for wood fiber/HDPE/nanoclay composites with respect to preparation method of the composites, and clay contents (weight ratio of PE-g-MAn to clay = 9.0).

Flame retardancy testing

The flame-retarding test was carried out according to ASTM D635. The measured data was equivalent to the burning rate of the material. The dimensions of the specimens used were 127 mm × 12.7 mm × 3.0 mm. The burning rate was calculated according to the formula

$$B = 60 \times \frac{D}{T} \quad (2)$$

where B is the burning rate in millimeters per minute; D is the length the flame travels (75 mm); and T is the time in seconds for the flame to travel the distance D. Five measurements per sample were taken to confirm the repeatability of the data.

RESULTS AND DISCUSSION

Structure characterization

Figure 1 compares XRD patterns for the PE-g-MAn–based clay masterbatch, the wood fiber/clay/HDPE composites made from this masterbatch, and the composites made by a direct mixing process with different clay contents. Shifting of the XRD peak towards lower angles than that of pure clay was apparent for all composites made by direct mixing processes regardless of the PE-g-MAn content, indicating the presence of an intercalated structure. In contrast, XRD characteristic peaks disappeared for the clay masterbatch, as well as for the 1, 3, and 5% clay composites made from it, suggesting that a high degree of an exfoliated structure was formed.

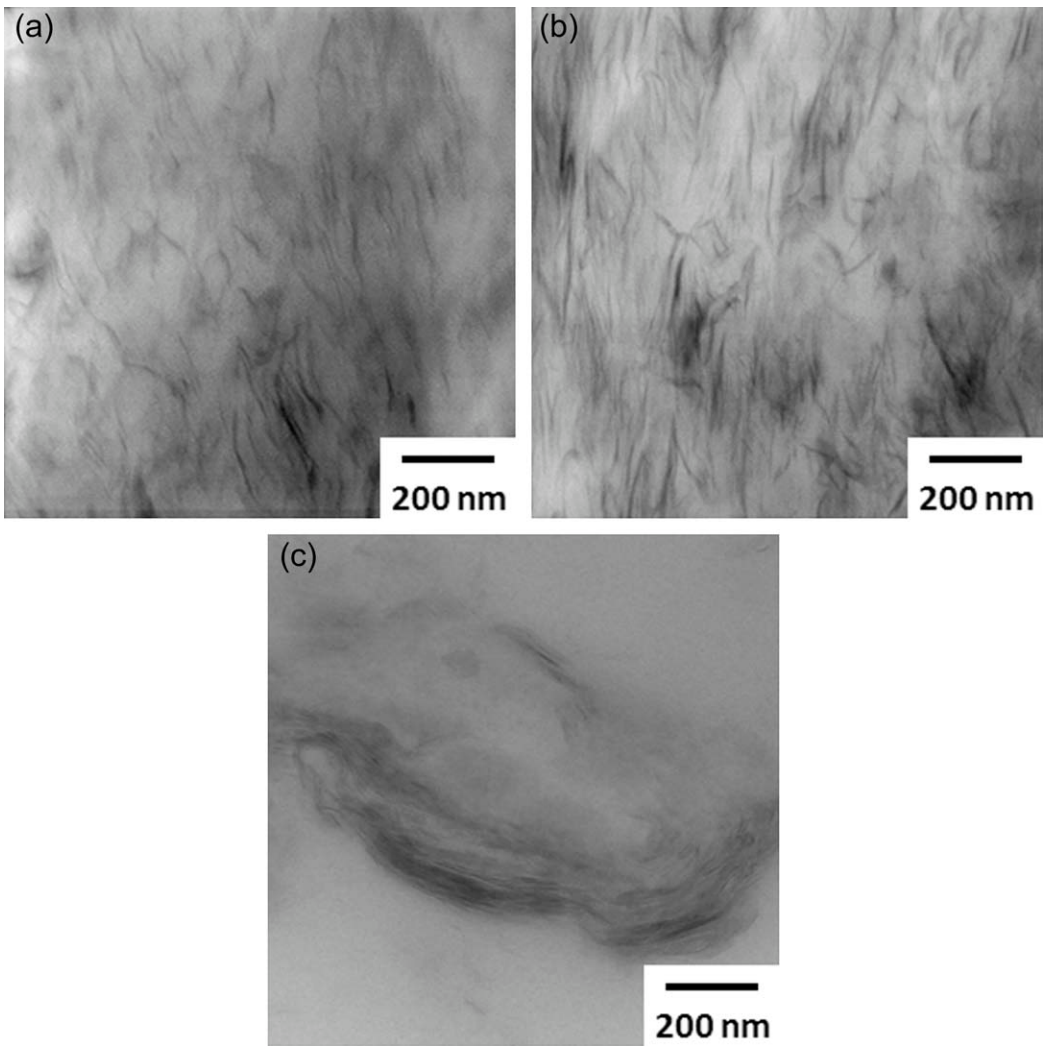

Figure 2 TEM micrographs of (a) 3% clay/wood fiber (30%)/HDPE nanocomposites melt-blended by masterbatch method, (b) 5% clay/wood fiber (30%)/HDPE nanocomposites melt-blended by masterbatch method, and (c) 5% clay/wood fiber (30%)/HDPE nanocomposites by direct melt blending.

Morphology characterization

Figure 2 shows the TEM images of two clay-filled WPCs (3 wt % (a) and 5 wt % (b) clay) melt-blended by masterbatch method, and one 5% clay-filled WPC by direct melt blending (c), which correspond to the XRD patterns presented in Figure 1. The white and the black represent the matrix phase and the clay particles, respectively. It is evident that for the nanocomposites melt-blended by masterbatch, nanosized individual silicate layers were well-dispersed randomly throughout the HDPE matrix. However, the 5% clay/wood fiber nanocomposite by direct blending shows some clay stacks with a few layers in certain regions, indicating an intercalated structure. Dennis et al.[11] stated that in the presence of PE-g-MAn, the primary clay particles (aggregates) are first fractured by mechanical shear in the extruder. The PE-g-MAn chains then diffuse into the clay galleries, due to a physical or chemical affinity between the polymer and the organoclay surface, and push the platelets apart. After this, an onion-like delaminating process continues to disperse the platelets into the HDPE matrix.

Rheological behavior

It has been reported that adding nanosized clay particles into pure polymers changes the rheological properties of the polymer matrix.[18–25] The rheological properties of nanocomposites are of particular importance because these properties relate to the nanocomposites' microstructure and determine their processability. Figure 3 illustrates the frequency dependence of G' and η^* for pure HDPE (a) and wood fiber/HDPE composites with intercalated and exfoliated clay of 1 wt % (b), 3 wt %

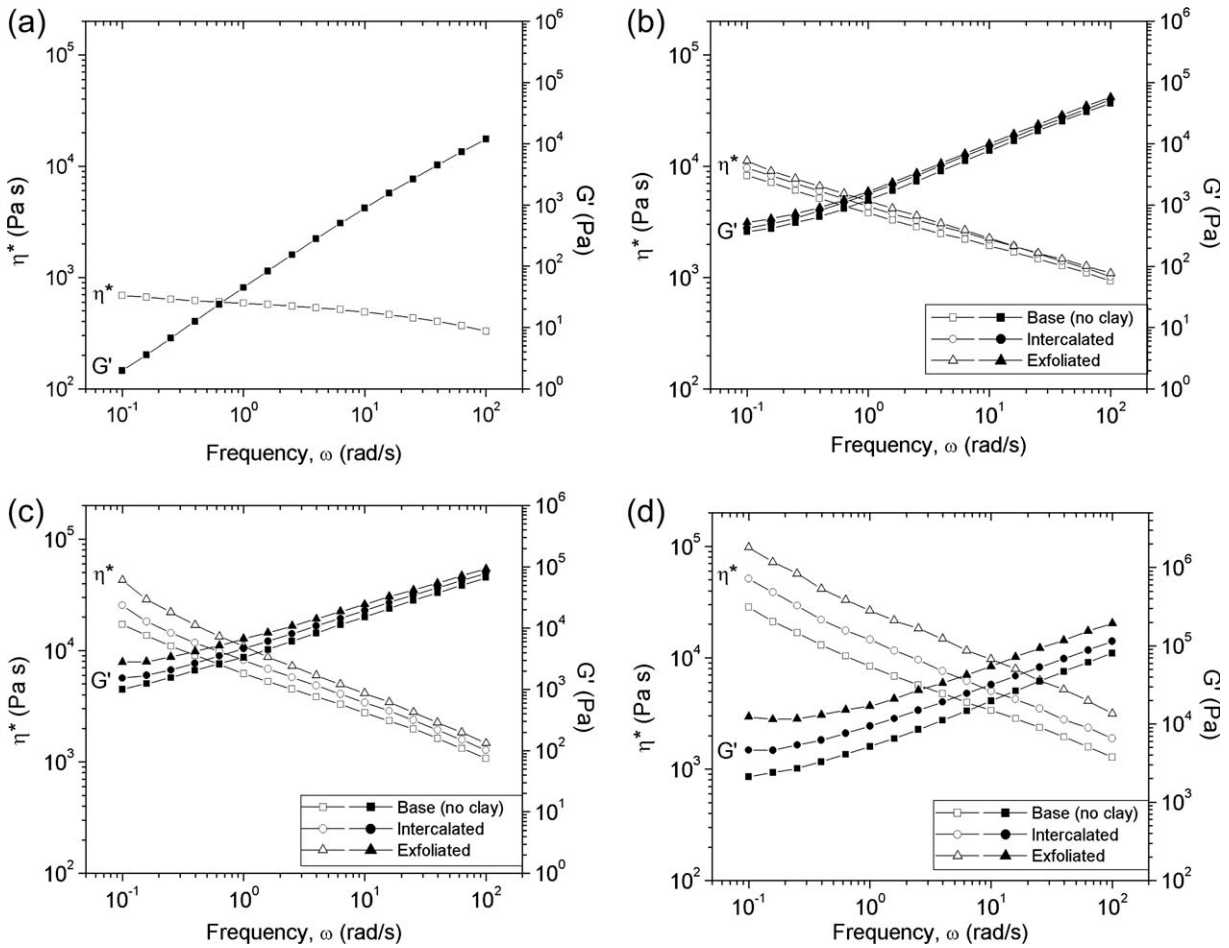

Figure 3 The effects of clay dispersion on G′ and η* of HDPE and wood fiber/HDPE nanocomposites with (a) pure HDPE, (b) 1 wt % clay, (c) 3 wt % clay, and (d) 5 wt % clay (weight ratio of PE-g-MAn to clay = 9.0).

(c), and 5 wt % (d), in which the weight ratio of PE-g-MAn to clay was 9.0. For comparison, the data for the respective composites without clay is also included. The absence of Newtonian plateau and the pronounced shear thinning of the WPCs are due largely to the presence of 30 wt % wood. The different composite structures are clearly reflected in the rheological behavior. The η* value of the wood fiber/HDPE composites increased in the presence of clay, accompanied by an increase in shear-thinning behavior. The effect of clay dispersion and clay content on complex viscosity is readily identified in Figure 4. The relative viscosity ratio of the exfoliated clay-filled samples increased more steeply as a function of clay content than that of the intercalated samples. Generally, the ratio of complex viscosities depends on the content, size, shape, and stiffness of the fillers.[29] In this study, the aspect ratio of the clay particles dispersed in the polymer matrix played an important role. The high aspect ratio and large surface area of the exfoliated clay particles was responsible for the higher ratio of relative viscosities observed in Figure 4. The high aspect ratio and large surface area cause a higher fraction of polymer chains to be confined by nanoplatelets; in turn, the mobility of the polymer chains is restricted.

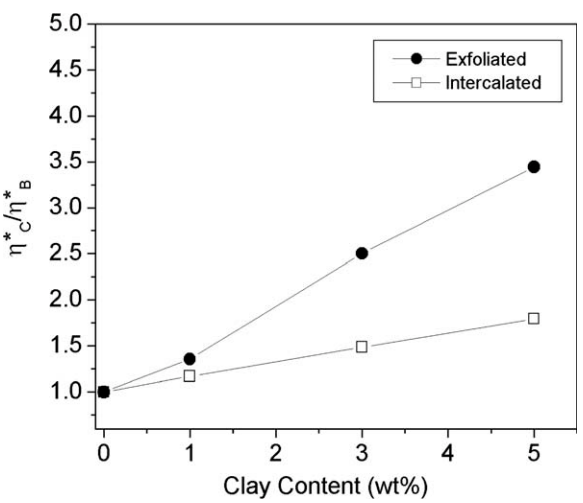

Figure 4 The ratio of complex viscosity of intercalated and exfoliated clay-filled composites (η^*_C) over that of their respective base composites (η^*_B) at a frequency (ω) of 0.1 rad/s.

TABLE II
Melting and Crystallization Parameters of Selected HDPE and Composites

Sample	T_m (°C)	T_c (°C)	ΔH_{exp} (J/g)	χ_c (%)
HDPE	128.3	113.4	191.8	65.50
No clay WPC	130.1 ± 0.3	117.5 ± 0.1	112.6 ± 0.7	54.93 ± 0.35
5% intercalated clay filled WPC	129.0 ± 0.3	118.2 ± 0.4	98.9 ± 3.0	51.90 ± 2.04
5% exfoliated clay filled WPC	129.2 ± 0.1	118.6 ± 0.1	100.9 ± 1.1	52.97 ± 0.60

The G' value of the clay-filled wood fiber/HDPE composites increased monotonically with improving clay dispersion in all frequency ranges. Moreover, the G' of composites with 3 wt % and 5 wt % clay tended to reach a plateau near a frequency of 0.1 rad/s, illustrating their pseudo-solid behavior. A similar behavior was observed for other polymer nanocomposites, such as the functionalized block-copolymer and polycarbonate.[30,31]

Crystallization behavior

The variation in the rate or degree of crystallization may be affected by the extent to which polymer chains undergo intercalation in the silicate interlayer spacing, and nanoparticles are dispersed in the polymer matrix; mechanical properties and various other nanocomposite characteristics in turn can be affected. Table II summarize the crystallization behaviors of the neat HDPE and composites with different levels of clay dispersion (5% clay) and all base materials (melting and crystallization temperature, ΔH_{exp}, and crystallinity). It seems that the presence of 5% clay had only a small effect on the crystallization temperature and crystallinity, compared to these same properties of base WPCs without clay. Furthermore, the selected composites were not influenced significantly by the degree of clay dispersion. On the other hand, the WPC without clay presented an increase in crystallization temperature (T_c) and a decrease in crystallinity with respect to those for the neat HDPE. This result may stem from the wood fibers acting as a nucleating agent in the polymer matrix during the nucleation stage, resulting in an increase in the crystallization temperature with increasing fiber content.[32–34] However, the fiber particles interfered more dominantly with the crystallization during the crystal growth, which resulted in a decreasing overall crystallinity level of the polymer with increasing fiber content. Such a decrease of crystallinity due to the addition of wood fiber may mask any effect of nanoclays on the crystallinity.

Mechanical properties

Figure 5 presents the tensile modulus (a) and flexural modulus (b) of the clay-filled wood fiber/HDPE composites, in which the weight ratio of PE-g-MAn to clay was 9.0, for various clay contents and degrees of clay dispersion. The base materials were wood fiber/HDPE composites that contained three different amounts of PE-g-MAn (9 wt %, 27 wt %, and 45 wt % of the composites), which were identical to amounts of PE-g-MAn in WPCs with clay (1 wt %, 3 wt %, and 5 wt % clay, respectively). For the composites, the extent to which the modulus improved depended directly on the thickness of the dispersed filler particles, and thus on the aspect

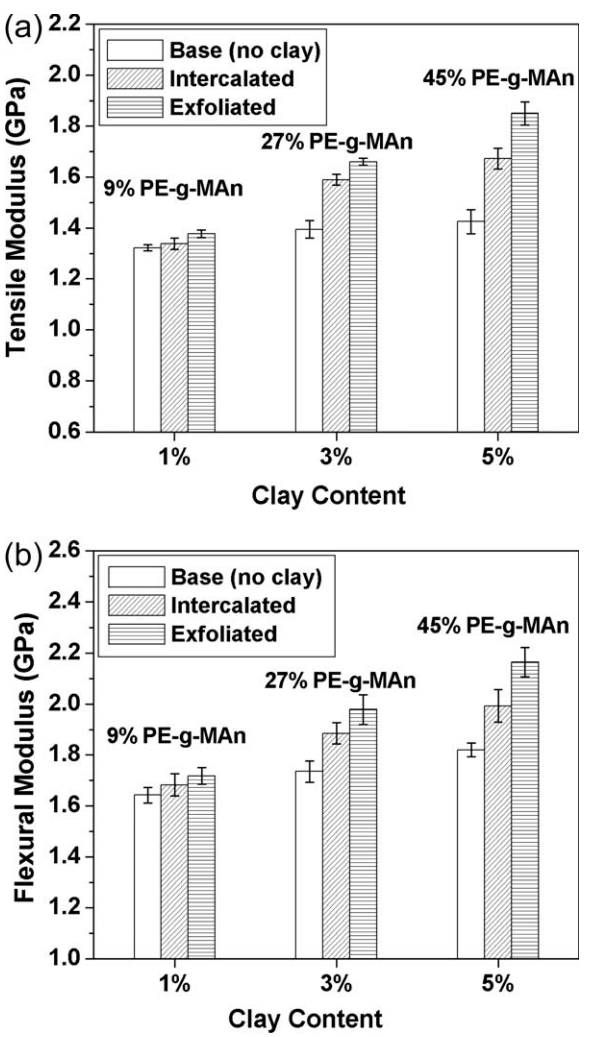

Figure 5 The effects of clay dispersion on the (a) tensile modulus and (b) flexural modulus of wood fiber/HDPE/clay nanocomposites (weight ratio of PE-g-MAn to clay = 9.0).

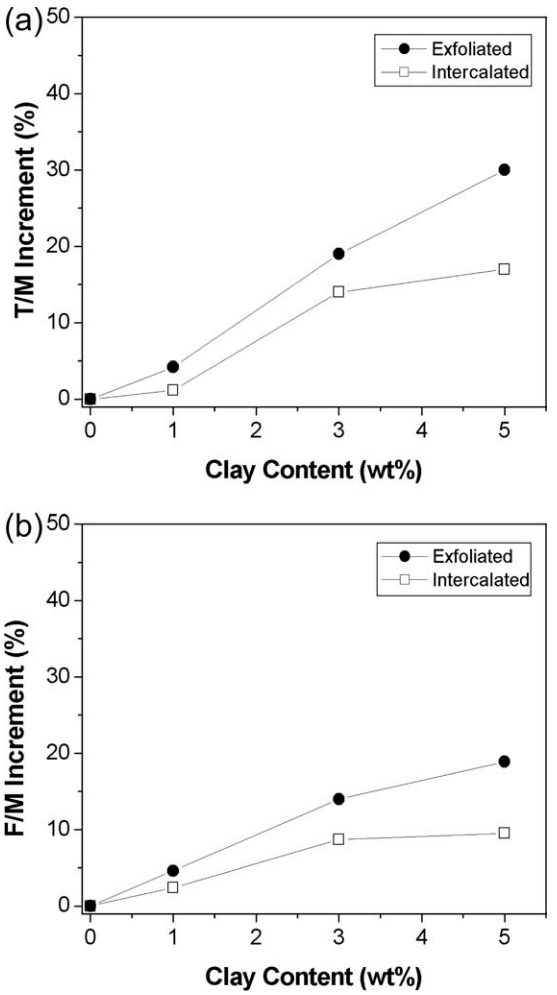

Figure 6 The increments in (a) tensile modulus and (b) flexural modulus of wood fiber/HDPE/clay nanocomposites with respect to their respective base composites with the increase of level of clay dispersion and clay content.

ratio.[35] As shown in Figure 5, the increase in the tensile and flexural moduli of WPCs in the presence of nanoclay was significant in comparison to the base WPCs without clay, despite the lower crystallinity. Moreover, Figure 6 shows that the difference in the degree of clay dispersion strongly influenced the final tensile modulus (a) and flexural modulus (b) of the composites as the clay content was increased, indicating that the improved stiffness was attributable to the exfoliated clay particles. On the other hand, intercalated particles, which have a lower number of dispersed particles, played a less significant role. It is therefore clear that the essential factor governing the enhancement of modulus in the nanocomposites is the large interfacial area between polymer and clay, generated by the high aspect ratio of the dispersed clay particles. The large interfacial area leads to better stress transfer at the interface between the HDPE matrix and the clay particles.

Figure 7 shows the influence of nanoclay and its dispersion on the tensile strength (a) of WPCs. Unlike the modulus, there were no significant differences across the composite samples between the two types of clay dispersion. Nevertheless, the addition of clay caused a slight increase in the flexural strength (b) at a high content of clay (3–5%). Furthermore, the better the clay dispersion, the higher the flexural strength, albeit only slightly. Figure 8 illustrates the notched Izod impact strength of clay-filled and unfilled (base) wood fiber/HDPE composites in which the weight ratio of PE-g-MAn to clay was 9.0, at various clay contents and degrees of clay dispersion. Contrary to the modulus improvement that occurred for WPCs in the presence of clay, the addition of clay decreased the notched Izod impact strength regardless of clay dispersion, particularly when the clay content was 3% or higher. This may be because the addition of clay decreased the ductility of the WPCs. However, the impact strength of

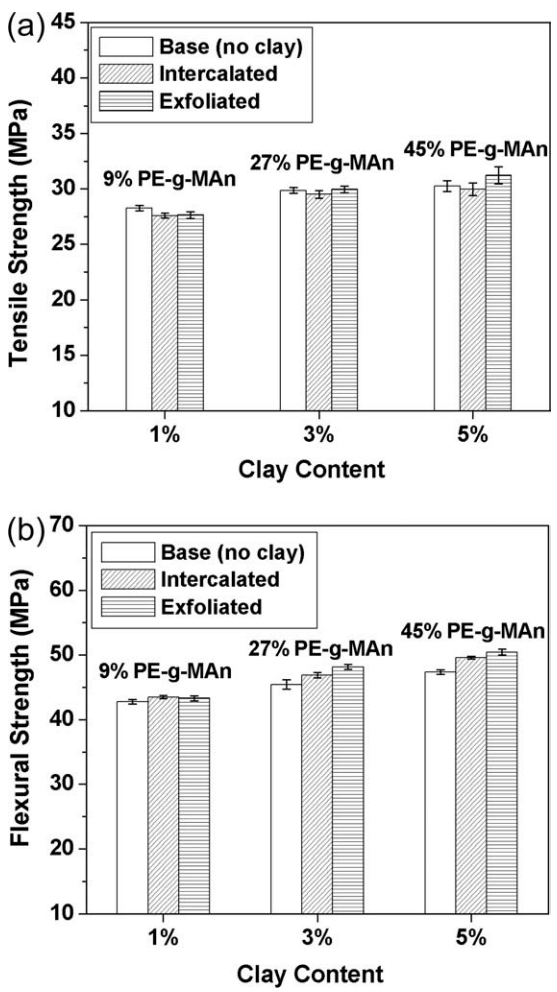

Figure 7 The effects of clay dispersion on the (a) tensile strength and (b) flexural strength of wood fiber/HDPE/clay nanocomposites (weight ratio of PE-g-MAn to clay = 9.0).

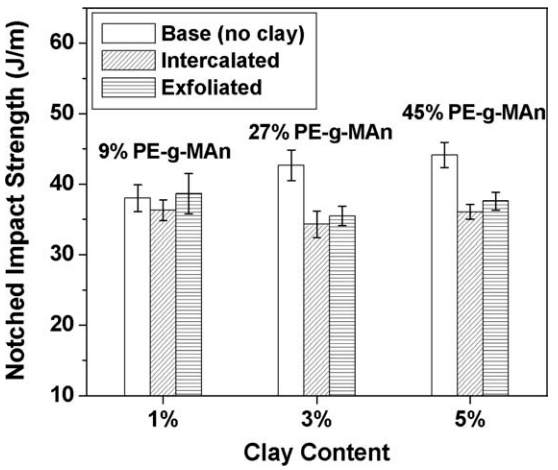

Figure 8 The effect of clay dispersion on the notched Izod impact strength of wood fiber/ HDPE/clay nanocomposites (weight ratio of PE-g-MAn to clay = 9.0).

exfoliated clay-filled WPCs was higher than that of intercalated WPCs for all clay contents. This may be due to the higher strength of exfoliated clay-filled WPCs (see Fig. 7).

Flame retarding properties

Figure 9 shows the burning rate of clay-filled and unfilled (base) wood fiber/HDPE composites for various clay contents and degrees of clay dispersion. The burning rate decreased for all composites in the presence of clay, but especially so for the exfoliated clay-filled composites (e.g., 27% decrease over the base material at 5 wt % clay). As shown in Figure 10, these composites exhibited a sharper decrease than intercalated clay-filled composites (e.g., 16% decrease over the base material at 5 wt % clay) as the clay content increased, indicating a significant

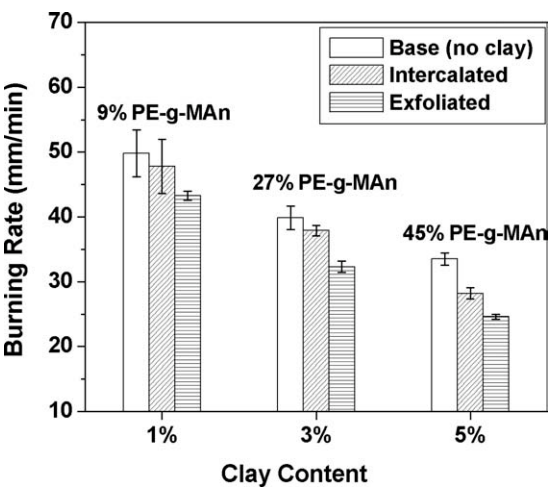

Figure 9 The effect of clay dispersion on the burning rate of wood fiber/HDPE/clay (weight ratio of PE-g-MAn to clay = 9.0).

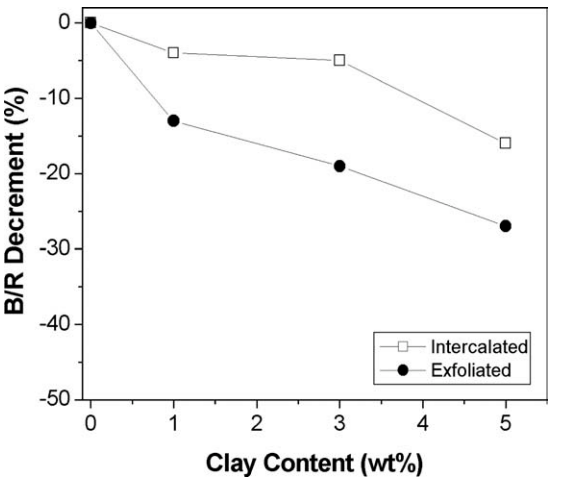

Figure 10 The decrements in burning rate of wood fiber/ HDPE/clay nanocomposites with respect to their respective base composites with the increase of level of clay dispersion and clay content.

improvement in flame-retarding performance. Consequently, we suggest that achieving a higher degree of exfoliation of nanoclay is the key to enhance the flame retarding properties of WPCs, when a small amount of clay is used. Gilman et al.[36] reported that the clay must be nanodispersed to retard the flammability of nanocomposites. In general, the flame retardant mechanism of the clay nanocomposites involves the formation of a high-performance carbonaceous-silicate char, which builds up on the surface during burning. This insulates the underlying material and slows the mass loss and energy release rate of the decomposition products. In addition, as aforementioned, well-dispersed nanoclays showed a strong increase in melt viscosity of the WPCs for even low contents, especially when low shear rates were applied. Accordingly, the nanodispersion resulted in structures that strongly reduce melt dripping, which in turn prevented rapid burning through dripping in this system, for more combustible material remaining in the pyrolysis zone.

On the other hand, as shown in Figure 9, the burning rate decreased gradually when the PE-g-MAn content increased in all base composites in the absence of clay. This may be due to the overall enhanced melt viscosity when the amount of PE-g-MAn is increased.[37]

CONCLUSIONS

In this study, well-exfoliated clay/wood fiber/HDPE nanocomposites were successfully created using a two-step melt-blending process using a PE-g-MAn–based nanoclay masterbatch. Exfoliated nanoclay-filled wood fiber/HDPE composites showed greater improvements in tensile and flexural moduli and

flame retardancy, with respect to composites without clay, than did intercalated clay-filled composites. Consequently, it was determined that achieving a higher degree of exfoliation for nanosized clay particles is integral to enhance the mechanical properties and flame retardancy of WPCs, when small amounts of clay (3–5%) are used.

The authors thank DuPont Canada, American Wood Fibers, and Nova Chemicals for supplying materials.

References

1. Oksman, K.; Sain, M., Eds. Wood-Polymer Composites; Woodhead Publishing: Cambridge, 2008.
2. Clemons, C. Forest Prod J 2002, 52, 10.
3. Balasuriya, P.; Ye, L.; Mai, Y.; Wu, J. J Appl Polym Sci 2002, 83, 2505.
4. Kokta, B. V.; Maldas, D.; Daneault, C.; Beland, P. Polym Plast Technol Eng 1990, 29, 87.
5. Bledzki, A. K.; Gassan, J. Prog Polym Sci 1999, 24, 221.
6. Pape, P. G.; Romenesko, D. J. J Vinyl Addit Technol 1997, 3, 225.
7. Le Bras, M.; Wilkie, C. A.; Bourbigot, S.; Duquesne, S.; Jama, C. Fire Retardancy of Polymers: New Applications of Mineral Fillers; Royal Society of Chemistry: Cambridge, 2005; Chapter 2.
8. Giannelis, E. P. Adv Mater 1996, 8, 29.
9. Krishnamoorti, E.; Vaia, R. A.; Giannelis, E. P. Chem Mater 1996, 8, 1718.
10. Kojima, Y.; Usuki, A.; Kawasumi, M.; Okada, A.; Fukushima, Y.; Kurauchi, T.; Kamigaito, O. J Mater Res 1993, 8, 1185.
11. Dennis, H. R.; Hunter, D. L.; Chang, D.; Kim, S.; White, J. L.; Cho, J. W.; Paul, D. R. Polymer 2001, 42, 9513.
12. Pavlidoua, S.; Papaspyridesb, C. D. Prog Polym Sci 2008, 33, 1119.
13. Saul, S. V.; Maria, L. L. Q.; Eduardo, R. V.; Francisco, J. M. R.; Juan, M. G. R. Macromol Mater Eng 2006, 291, 128.
14. Truss, R. W.; Yeow, T. K. J Appl Polym Sci 2006, 100, 3044.
15. Osman, M. A.; Rupp, J. E. P.; Suter, U. W. Polymer 2005, 46, 8202.
16. Xu, Y.; Fang, Z.; Tong, L. J Appl Polym Sci 2005, 96, 2429.
17. Chrissopoulou, K.; Altintzi, I.; Anastasiadis, S. H.; Giannelis, E. P.; Pitsikalis, M.; Hadjichristidis, N.; Theophilou, N. Polymer 2005, 46, 12440.
18. Lee, Y. H.; Park, C. B.; Wang, K. H. J Cell Plast 2005, 41, 487.
19. Lee, J. A.; Kontopoulou, M.; Parent, J. S. Polymer 2004, 45, 6595.
20. Liang, G.; Xu, J.; Bao, S.; Xu, W. J Appl Polym Sci 2004, 91, 3974.
21. Hotta, S.; Paul, D. R. Polymer 2004, 45, 7639.
22. Kato, M.; Okamoto, H.; Hasegawa, N.; Tsukigase, A.; Usuki, A. Polym Eng Sci 2003, 43, 1312.
23. Gopakumar, T. G.; Lee, J. A.; Kontopoulou, M.; Parent, J. S. Polymer 2002, 43, 5483.
24. Koo, C. M.; Ham, H. T.; Kim, S. O.; Wang, K. H.; Chung, I. J.; Kim, D. C.; Zin, W. C. Macromolecules 2002, 35, 5116.
25. Lee, Y. H.; Park, C. B.; Sain, M.; Kontopoulou, M.; Zheng, W. G. J Appl Polym Sci 2007, 105, 1993.
26. Lee, Y. H.; Wang, K. H.; Park, C. B.; Sain, M. J Appl Polym Sci 2007, 103, 2129.
27. Guo, G.; Wang, K. H.; Park, C. B.; Kim, Y. S.; Li, G. J Appl Polym Sci 2007, 104, 1058.
28. Guo, G.; Park, C. B.; Lee, Y. H.; Kim, Y. S.; Sain, M. Polym Eng Sci 2007, 47, 330.
29. Shenoy, A. V. Rheology of Filled Polymer System; Kluwer Academic Publishers: Dordrecht, 1999.
30. Ren, J. A.; Silva, S.; Krishnamoorti, R. Macromolecules 2000, 39, 3979.
31. Lee, K. M.; Han, C. D. Macromolecules 2003, 36, 804.
32. Sombatsompop, N.; Kositchaiyong, A.; Wimolmala, E. J Appl Polym Sci 2006, 102, 1896.
33. Colom, X.; Canvate, J.; Pages, P.; Saurina, J.; Carrasco, F. J Rein Plast Comp 2000, 19, 818.
34. Ganan, P.; Mondragon, I. J Therm Anal Calorim 2003, 73, 783.
35. Nielsen, L. E.; Landel, R. F. Mechanical Properties of Polymers and Composites, 2nd ed.; Marcel Deckker, 1994.
36. Gilman, J. W.; Jackson, C. L.; Morgan, A. B.; Harris, J. R.; Manias, E.; Giannelis, E. P.; Wuthenow, M.; Hilton, D.; Philips, S. H. Chem Mater 2000, 12, 1866.
37. Anna, P.; Marosi, G.; Bourbigot, S.; Le Bras, M.; Delobel, R. Polym Degrad Stab 2002, 77, 243.